Improving the Processing Efficiency of Femtosecond Laser Sulfur Hyperdoping of Silicon by Diffractive Beam Shaping

Patrick Mc Kearney*, Ingo Lebershausen, Sören Schäfer, Simon Paulus, and Stefan Kontermann

Institute for Microtechnologies (IMtech), University of Applied Sciences RheinMain, Am Brückweg 26, 65428 Rüsselsheim
Corresponding author's e-mail: Patrick.McKearney@hs-rm.de

We demonstrate and compare two approaches for reducing processing time for ultrashort pulse laser surface functionalization with application to femtosecond laser hyperdoping of silicon with a laser pulse duration of 800 fs and an irradiation wavelength of 1030 nm. In the first, we use a Gaussian intensity distribution and increase the repetition rate from 1 kHz to 1002 kHz while keeping all other parameters and thus the accumulated fluence constant. We find that the sub-bandgap absorptance of the material, which we take as target measure, decreases above a repetition rate of 250 kHz. This suggests an inherent limitation of this approach. The second approach is characterized by the use of a line-shaped intensity distribution which is achieved by diffractive beam shaping using a phase-only spatial light modulator. This process proves to be suitable for laser hyperdoping of silicon with a 22-fold enhanced area processing rate while maintaining a sub-bandgap absorptance of above 80 $\%_{abs}$.

DOI: 10.2961/jlmn.2023.02.2003
Keywords: femtosecond-laser hyperdoping, black silicon, beam shaping, spatial light modulator, processing efficiency

1. Introduction

The average power of ultrashort pulse (USP) laser sources has increased steadily over the past decade [1–4] and the maximum processing rate scales linearly with the average power as demonstrated in the work of Neuenschwander et al. [5,6]. However, switching to higher power laser sources calls for an adaption of USP processes developed on conventional setups. Since the average power in USP processing results from the product of energy and frequency, it can be enhanced by increasing one of the two parameters.

Processing at high repetition rates in combination with high scanning speed allows to increase the average power. At repetition rates of several hundred kHz detrimental effects such as pulse to pulse interactions [7,8] as well as heat accumulation [9–13] must be considered and may cause a limitation regarding the trade-off between processing speed and targeted material quality.

Alternatively, the pulse energy is redistributed to a larger area [14], like for example in a top-hat distribution [18], by beam splitting [15] or a combination of both [18], and thus the average power is increased while maintaining the peak fluence.

Using a phase-only liquid-crystal-on-chip spatial light modulator (LCoS-SLM) allows to modulate the intensity distribution in the focal plane by using computer generated holograms (CGHs) [15,19–21]. The calculation of CGHs can be addressed by iterative algorithms, such as the Gerchberg-Saxton algorithm [16], or by analytical solutions [17].

Processing of silicon with ultrashort laser pulses induces the formation of laser-induced periodic surface structures (LIPSS) which turn into light trapping structures if high pulse densities are used [22–25]. If this process takes place under sulfur-hexafluoride SF_6 atmosphere, sulfur dopants get incorporated into the lattice beyond the thermal solubility limit [26–28]. The resulting material, referred to as laser hyperdoped black silicon, exhibits high above- and sub-bandgap absorptance and is of interest for silicon-based infrared sensitive optoelectronic devices.

This work demonstrates the possibilities and limitations of increasing the processing speed of laser hyperdoping of silicon when using a Gaussian intensity distribution. Furthermore, it shows an approach based of diffractive beam shaping to overcome these limitations and achieve higher surface processing rates while maintaining the high sub-bandgap absorptance.

2. Experimental

We perform sulfur hyperdoping on p-type CZ silicon (100) by irradiation with ultrashort laser pulses under SF_6 atmosphere at a pressure of 675 mbar. The Yb:YAG laser source (Amplitude, Tangor 100) emits pulses with a central wavelength of 1030 nm and a pulse duration of τ = 800 fs. The pulses are guided through a phase-only LCoS-SLM based beam shaping system (Pulsar Photonics, Flexible Beam Shaper G3), deflected by a two-axis galvanometer scanner and focused by an f-theta objective (f = 340 mm) to a Gaussian distribution with a $1/e^2$ diameter of $2w_0$ = 106 µm in the processing plane. A phase mask based on the hyperbolic phase function [29] is used to create a line-shaped intensity distribution with 1 mm in width and 106 µm in height, measured by a camera-based beam profiling system. We set the peak fluence to Φ_0 = 0.35 J/cm² for the Gaussian intensity distribution. The pulses are scanned across the wafer surface with a scan line distance d_{Line} 4.2 µm as illustrated in Figure 1. When increasing the repetition rate from 1 kHz to 1002 kHz, the scanning veloc-

ity was adapted to maintain a pulse-to-pulse distance of d_{Pulse} = 4.2 µm and a pulse density of 500 pulses per spot. The resulting pulse overlap in scan direction and perpendicular to it is 96 %.

Processing with the line-shaped intensity distribution is carried with a pulse energy of E_P = 316 µJ, resulting in a fluence of Φ = 0.32 J/cm². The repetition rate is f_{Rep} = 200 kHz and the scanning velocity v_{Scan} = 5000 mm/s, resulting in d_{Pulse} = 25 µm and a pulse overlap of 76 %. The scan direction is perpendicular to the long side of the line profile as illustrated in Figure 1 and the scan line distance is varied from 10 to 40 µm in steps of 5 µm, which corresponds to a line overlap of 96 % to 99 %. In contrast to processing with the Gaussian beam, the direction of the scan vector remains the same. In this way, macroscopic periodic structures, which occur due to the direction dependence of the ablation of the line profile, are avoided.

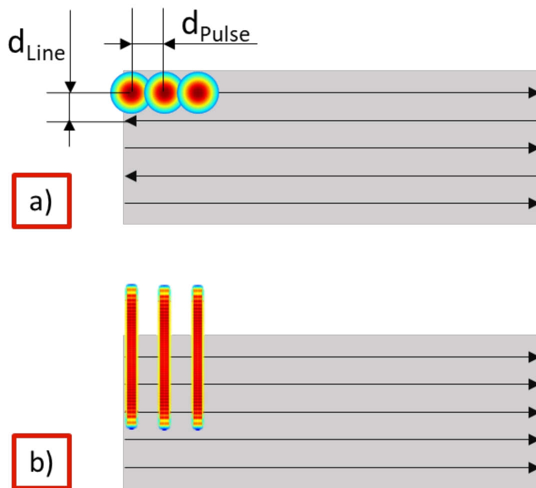

Fig. 1 Machining strategy for processing with a Gaussian (a) and a line-shaped (b) intensity distribution.

We measure the optical transmission T and reflectance R from 250 to 2250 nm with a spectrophotometer (Perkin Elmer Lambda 750) with an integrating sphere and calculate the absorptance by $A = 1 - R - T$.

The surface morphology is investigated by scanning electron microscopy (JEOL JSM-6380LV) under an incident angle of 30°.

3. Results and Discussion

Laser processing of silicon results in increased surface roughness, which is attributed to the formation of LIPSS during processing above the threshold fluence for ablation, which is below 0.2 J/cm² [23, 30] for comparable laser parameters [31]. In addition, the rapid melting and solidification [32] of the near-surface layers leads to hyperdoping with sulfur, resulting in sub-bandgap absorptance of up to 90%, as shown in Figure 2. When the repetition rate is increased from 1 kHz up to 250 kHz, the above-bandgap absorptance decreases, as reported by Nava et al. [33]. The change in sub-bandgap absorptance in this regime is negligible.

For repetition rates from 250 kHz to 1002 kHz we observe a decrease of above- and sub-bandgap absorptance towards higher repetition rates. We attribute this to less pronounced light-trapping structures, which is in good agreement with the SEM images in Figure 5 (a-f). Since this effect is more pronounced with increasing repetition rate, we consider pulse-to-pulse interactions to be the cause. Interaction with the plasma or ablated material of the previous pulse can lead to shielding of the following pulse [7] and thus to a reduction of the energy absorbed by the surface. Heat accumulation can lead to re-melting of the structured surface, which can be observed in Figure 5 (f). This results in less pronounced light-trapping structures, which lead to a decrease in absorptance in the entire spectral range.

From these results we conclude, that up-scaling of laser hyperdoping by increasing the repetition rate and scanning velocity is limited, when aiming for high sub-bandgap absorptance. Furthermore, the results show that the specification of the used repetition rate, in addition to pulse density and peak fluence, becomes important especially for f_{Rep} > 250 kHz.

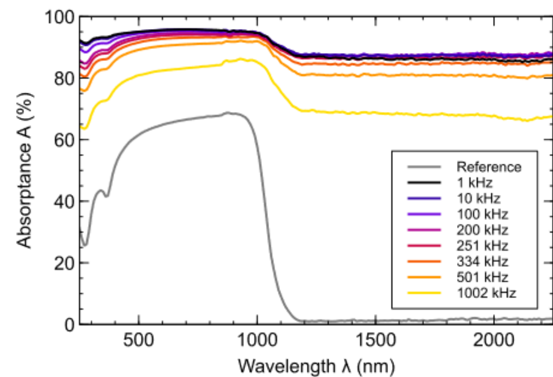

Fig. 2 Absorptance after processing with Gaussian beam with repetition rates from 1 kHz to 1002 kHz. The line distance and the pulse-to-pulse distance were set to d_{Pulse} = d_{Line} = 2.7.

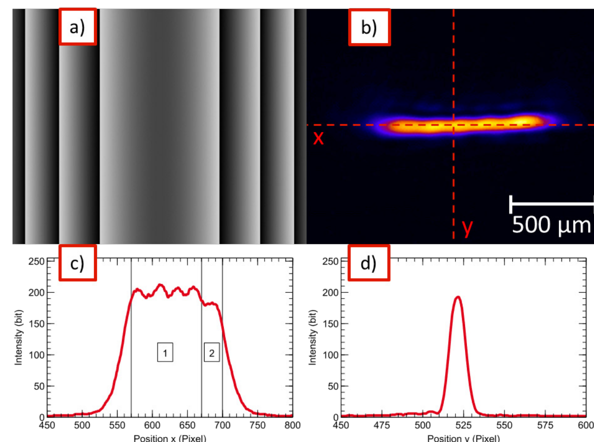

Fig. 3 CGH calculated with the hyperbolic phase function (a), intensity distribution in the focal plane (b) and the intensity profiles along the dashed lines (c, d).

Figure 3 shows the CGH calculated with the hyperbolic phase function (a), the intensity distribution in the focal plane (b), and the intensity profiles along the plotted x (c) and y (d) axes. Figure 3 (b) shows a slight curvature of the line profile as well as inhomogeneities along the x axes. These can be seen in the profile in Figure 3 (d) by local minima and maxima. The uniformity according to [34] is

0.81 in interval 1 and 0.93 in the combined intervals 1 and 2 in Figure 3 (c). A possible cause for the drop of intensity in the right end of interval 1 is a non-ideal illumination of the SLM, which leads to a shift of intensity towards one axis of the distribution. The inhomogeneities in interval 2 can be caused by the incident intensity distribution or non-idealities of the SLM such as pixel crosstalk [35-37]. To reduce the possible effects of these inhomogeneities, we work with small line spacing and scan unidirectionally, as shown in Figure 1 (b).

Laser processing of silicon with a line-shaped intensity distribution leads to the comparable, but less pronounced surface structures as when processing with a Gaussian beam as shown in Figures 5 (g) and 5 (h). Furthermore, the material is hyperdoped with sulfur, which is indicated by the near-unity sub-bandgap absorptance. Figure 4 shows the optical absorptance spectra of hyperdoped silicon processed with a line-shaped intensity distribution at different scan line distances.

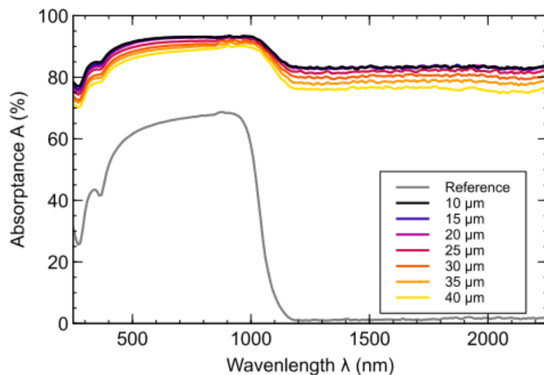

Fig. 4 Absorptance after processing at f_{rep} = 200 kHz with a line-shaped intensity distribution.

While line distances between 10 and 20 µm result in similar properties, the absorptance decreases towards higher line distances, which we attribute to the lower accumulated fluence. However, higher line distances result in lower processing times, leading to a trade-off between sub-bandgap absorptance and area processing rate $\dot{A}$.

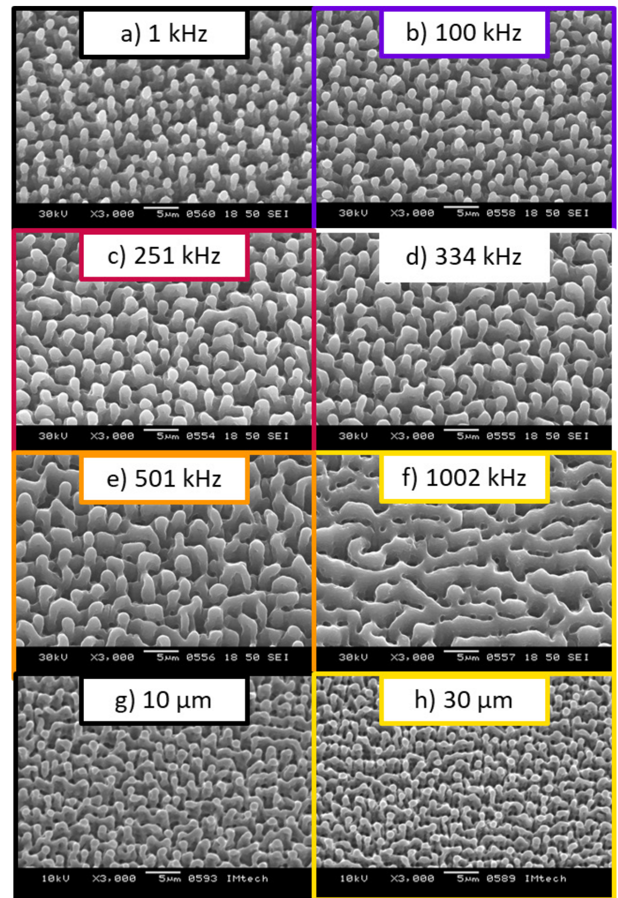

Fig. 5 SEM images of hyperdoped silicon after processing with Gaussian beam at different repetition rates (a – f) and with a line-shaped intensity distribution with a scan line distance of 10 µm (g) and 30 µm (h).

We plot the sub-bandgap absorptance at 1500 nm against the area processing rate in Figure 6 to compare both approaches in terms of processing efficiency. Processing with a Gaussian intensity distribution leads to an absorptance of 87 $\%_{abs}$ for processing rates below 5 mm²/s. Increasing the processing rate to 14 mm²/s results in a decrease in absorptance down to 69 $\%_{abs}$. With the system used in this work, this also represents the upper limit for the area processing rate, since the scanning speed is limited to 5000 mm/s. Processing with a line-shaped intensity distribution allows to increase the area processing rate to 167 mm²/s, or 100 cm²/min, while maintaining an absorptance of above 80 $\%_{abs}$.

Area processing rates reported so far are in the range of several 100 [38] to 2000 cm²/min [39]. Since the speed for these processes scales with the pulse energy, we normalize the surface machining rate to the applied pulse energy. The processes presented here achieve 0.32 with the same processing quality up to a maximum of 0.40 cm²/min·µJ and are slightly lower in comparison with 0.48 cm²/min·µJ [39] and 0.54 cm²/min·µJ [38] but in the same order of magnitude.

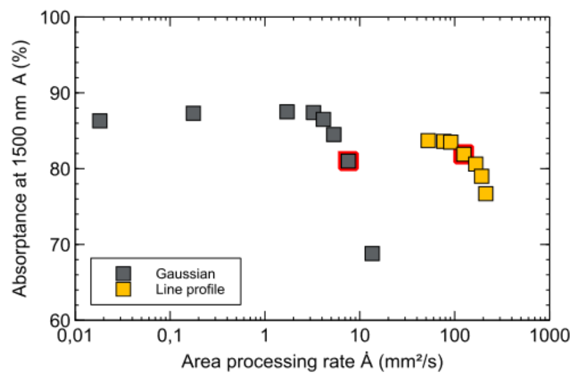

Fig. 6 Sub-bandgap absorptance at λ = 1500 nm versus area processing rate for processing with a Gaussian and a line-shaped intensity distribution. The data points highlighted in red are used to compare the two methods.

4. Conclusion

We presented two approaches for increasing the area processing rate for laser hyperdoping of silicon. The first approach is based on increasing repetition rate and scanning velocity while using a Gaussian intensity distribution while keeping all other parameters constant. In this way, we were able to increase the area processing rate from 0.02 mm²/s at 1 kHz to 3.25 mm²/s at 200 kHz, which corresponds to a factor of 163, while maintaining the optical properties of the hyperdoped material. Towards higher repetition rates and thus higher processing speed the sub-bandgap absorptance decreases sharply due to heat accumulation, which results in less pronounced light-trapping structures. To overcome this limitation, we used a line-shaped intensity distribution, created by diffractive beam shaping using an LCoS-SLM. This approach leads to comparable results in terms of sub-bandgap absorptance. When comparing processing parameters which lead to a sub-bandgap absorptance of 81 $\%_{abs}$ the area processing rate has been increased from 7.58 mm²/s with a Gaussian distribution at f_{rep} = 501 kHz to 166.67 mm²/s with the line-shaped intensity distribution with a line distance of 30 µm, which corresponds to a factor of 22.

Acknowledgments and Appendixes

This work was funded by the Federal Ministry of Education and Research of Germany under Grant No. FKZ 03INT701AA.

References

[1] P. Russbueldt, T. Mans, G. Rotarius, J. Weitenberg, H. D. Hoffmann, and R. Poprawe: Opt. Express, 17, (2009) 12230.
[2] P. Russbueldt, T. Mans, J. Weitenberg, H. D. Hoffmann, and R. Poprawe: Opt. Lett., 35, (2010) 4169.
[3] J.-P. Negel, A. Voss, M. Abdou Ahmed, D. Bauer, D. Sutter, A. Killi, and T. Graf: Opt. Lett., 38, (2013) 5442.
[4] F. Emaury, C. J. Saraceno, B. Debord, D. Ghosh, A. Diebold, F. Gèrôme, T. Südmeyer, F. Benabid, and U. Keller: Opt. Lett., 39, (2014) 6843.
[5] B. Neuenschwander, B. Jaeggi, M. Schmid, V. Rouffiange, and P.-E. Martin: Proc. SPIE, Vol. 8243, (2012) 824307.
[6] B. Neuenschwander, B. Jaeggi, M. Schmid, and G. Hennig: Phys. Procedia, 56, (2014) 1047.
[7] J. Finger and M. Reininghaus: Opt. Express, 22, (2014) 18790.
[8] J. Finger, C. Kalupka, and O. Nottrodt: Proc. ICALEO, (2016), M303.
[9] A. Ancona, F. Röser, K. Rademaker, J. Limpert, S. Nolte, and A. Tünnermann: Opt. Express, 16, (2008) 8958.
[10]J. Schille, R. Ebert, U. Loeschner, P. Scully, N. Goddard, and H. Exner: Proc. SPIE, Vol. 7589, (2010) 758915.
[11] F. Bauer, A. Michalowski, T. Kiedrowski, and S. Nolte: Opt. Express, 23, (2015) 1035.
[12]J. Finger, B. Bornschlegel, M. Reininghaus, A. Dohrn, M. Nießen, A. Gillner, and R. Poprawe: Adv. Opt. Technol., 7, (2018) 145.
[13] D. Haasler and J. Finger: J. Laser Appl., 31, (2019) 22201.
[14]M. Smarra, M. Janitzki, and K. Dickmann: Phys. Procedia, 83, (2016) 1145.
[15]J. Li, Y. Tang, Z. Kuang, J. Schille, U. Loeschner, W. Perrie, D. Liu, G. Dearden, and S. Edwardson: Opt. Lasers in Eng., 112, (2019) 59.
[16] Z. Kuang, D. Liu, W. Perrie, S. Edwardson, M. Sharp, E. Fearon, G. Dearden, and K. Watkins: Appl. Surf. Sci. 255, (2009) 6582.
[17]M. Kahle, D. Nodop, and J. Rücker: Proc. CIRP, Vol. 94, (2020) 807.
[18] C. Lutz, G.-L. Roth, S. Rung, C. Esen, and R. Hellmann: J. Laser Micro Nanoeng., 16, (2021) 62-67.
[19]J. Finger and M. Hesker: J. Phys. Photonics, 3, (2021) 21004.
[20]R. W. Gerchberg and W. O. Saxton: Optik, (1972) 237.
[21]H. Aagedal, M. Schmid, S. Egner, J. Müller-Quade, T. Beth, and F. Wyrowski: J. Opt. Soc. Am. A, 14, (1997) 1549.
[22]J. E. Sipe, J. F. Young, J. S. Preston, and H. M. van Driel: Phys. Rev. B, 27, (1983) 1141.
[23]J. Bonse, S. Baudach, J. Krüger, W. Kautek, and M. Lenzner: Appl. Phys. A, 74, (2002) 19.
[24]J. Bonse and J. Krüger: J. Appl. Phys., 108, (2010) 34903.
[25]T.-H. Her, R. J. Finlay, C. Wu, S. Deliwala, and E. Mazur: Appl. Phys. Lett., 73, (1998) 1673.
[26]K.-M. Guenther, T. Gimpel, S. Kontermann, and W. Schade: Appl. Phys. Lett., 102, (2013) 202104.
[27]K. C. Phillips, H. H. Gandhi, E. Mazur, and S. K. Sundaram: Adv. Opt. Photon., 7, (2015) 684.
[28]J. M. Warrender: Appl. Phys. Rev., 3, (2016) 31104.
[29]D. Nodop, J. Ruecker, S. Waechter, and M. Kahle: Opt. Lett., 44, (2019) 2169.
[30]C. S. R. Nathala, A. Ajami, W. Husinsky, B. Farooq, S. I. Kudryashov, A. Daskalova, I. Bliznakova, and A. Assion: Appl. Phys. A, 122, (2016) 88.
[31]J. Bonse and S. Gräf: Laser Photonics Rev., 14, (2020) 2000215.
[32]M.-J. Sher, N. M. Mangan, M. J. Smith, Y.-T. Lin, S. Marbach, T. M. Schneider, S. Gradečak, M. P. Brenner, and E. Mazur: J. Appl. Phys., 117, (2015) 125301.
[33]G. Nava, R. Osellame, R. Ramponi, and K. C. Vishnubhatla: Opt. Mater. Express, 3, (2013) 612.
[34]R. Di Leonardo, F. Ianni, and G. Ruocco: Opt. Express, 15, (2007) 1913.

[35]M. Persson, D. Engström, and M. Goksör: Opt. Express, 20, (2012) 22334.
[36]B. Apter, U. Efron, and E. Bahat-Treidel: Appl. Opt., 43, (2004) 11.
[37]P. F. McManamon, T. A. Dorschner, D. L. Corkum, L. J. Friedman, D. S. Hobbs, M. Holz, S. Liberman, H. Q. Nguyen, D. P. Resler, R. C. Sharp, and E. A. Watson: Proceedings of the IEEE, 84, (1996) 268.
[38]S. Faas, U. Bielke, R. Weber, and T. Graf: Sci. Rep., 9, (2019) 1933.
[39]P. Hauschwitz, J. Martan, R. Bičišťová, C. Beltrami, D. Moskal, A. Brodsky, N. Kaplan, J. Mužík, D. Štepánková, J. Brajer, D. Rostohar, J. Kopeček, L. Prokešová, M. Honner, V. Lang, M. Smrž, and T. Mocek: Sci. Rep., 11, (2021) 22944.

(Received: February 27, 2023, Accepted: July 9, 2023)